Matter and Radiation at Extremes | RESEARCH ARTICLE | scitation.org/journal/mre

Universal Fermi velocity in highly compressed hydride superconductors

Cite as: Matter Radiat. Extremes **7**, 058403 (2022); doi: 10.1063/5.0091446
Submitted: 15 March 2022 • Accepted: 22 July 2022 •
Published Online: 23 August 2022

Evgeny F. Talantsev[a)]

AFFILIATIONS

M. N. Miheev Institute of Metal Physics, Ural Branch, Russian Academy of Sciences, 18, S. Kovalevskoy St., Ekaterinburg 620108, Russia and NANOTECH Centre, Ural Federal University, 19 Mira St., Ekaterinburg 620002, Russia

[a)]**Author to whom correspondence should be addressed:** evgney.talantsev@imp.uran.ru

ABSTRACT

The Fermi velocity v_F is one of the primary characteristics of any conductor, including any superconductor. For conductors at ambient pressure, several experimental techniques have been developed to measure v_F, and, for instance, Zhou *et al.* [Nature **423**, 398 (2003)] reported that high-T_c cuprates exhibited a universal nodal Fermi velocity $v_{F,\mathrm{univ}} = (2.7 \pm 0.5) \times 10^5$ m/s. However, there have been no measurements of v_F in highly compressed near-room-temperature superconductors (NRTS), owing to experimental challenges. Here, to answer the question of the existence of a universal Fermi velocity in NRTS materials, we analyze the full inventory of data on the ground-state upper critical field $B_{c2}(0)$ for these materials and find that this class of superconductors exhibits a universal Fermi velocity $v_{F,\mathrm{univ}} = (1/1.3) \times [2\Delta(0)/k_B T_c] \times 10^5$ m/s, where $\Delta(0)$ is the ground-state amplitude of the energy gap. The ratio $2\Delta(0)/k_B T_c$ varies within a narrow range $3.2 \leq 2\Delta(0)/k_B T_c \leq 5$, and so $v_{F,\mathrm{univ}}$ in NRTS materials lies in the range 2.5×10^5 m/s $\leq v_{F,\mathrm{univ}} \leq 3.8 \times 10^5$ m/s, which is similar to the range of values found for the high-T_c cuprate counterparts of these materials.

I. INTRODUCTION

Since pivotal experimental discovery of the first near-room-temperature superconductor (NRTS) H_3S by Drozdov *et al.*,[1] nearly two dozen highly compressed hydrogen-rich superconducting phases have been synthesized in binary and ternary systems.[2–17] Experimental studies of NRTS are well supported by first-principles calculations,[18–30] but experimental characterizations of NRTS phases are limited by the narrow range of techniques that are available for materials inside diamond anvil cells (DACs).[25–27] These comprise x-ray diffraction (XRD) phase analysis, Raman spectroscopy, and magnetoresistance measurements,[31–35] although, with the use of some advanced techniques, Hall effect measurements can also be performed.[31] Because of this, only two characteristic values of the superconducting state of the NRTS phases are commonly extracted from experimental data, namely, the transition temperature T_c and the extrapolated value for the ground-state upper critical field $B_{c2}(0)$ or the ground-state superconducting coherence length $\xi(0)$, which can be derived from the Ginzburg–Landau[36] expression

$$\xi(0) = \sqrt{\frac{\phi_0}{2\pi B_{c2}(0)}}, \tag{1}$$

where $\phi_0 = h/2e$ is the superconducting flux quantum, with h being Planck's constant and e the electric charge of the electron.

Other important parameters of NRTS materials, among which we can mention the Fermi velocity v_F, have not been measured to date, owing to the challenges of performing such measurements on samples inside DACs. However, considering that all NRTS superconductors are hydrides, there is an expectation that these materials will exhibit a universal Fermi velocity $v_{F,\mathrm{univ}}$, as has been discovered in cuprates, for which $v_{F,\mathrm{univ}} = (2.7 \pm 0.5) \times 10^5$ m/s, as reported by Zhou *et al.*[37] (see Fig. 1).

The theoretical motivation for the quest for a universal Fermi velocity in NRTS comes, on the one hand, from the recent understanding[38] that sulfur in H_3S is analogous to the oxygen in cuprates, and, on the other hand, from the fact that highly compressed hydrides fit nicely with the main global scaling laws for superconductors.[39–43] However, it should be noted that an analysis

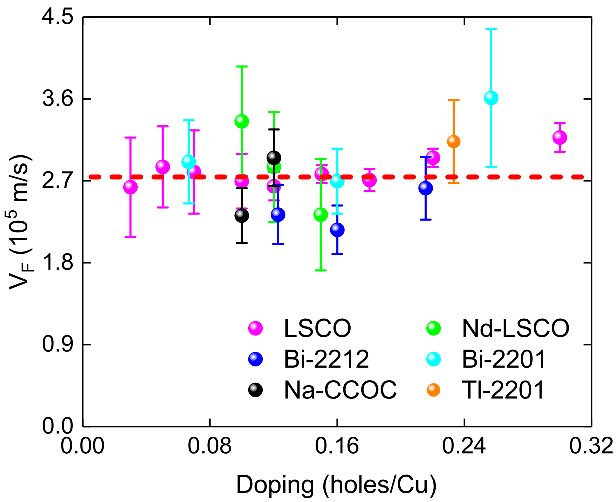

FIG. 1. Universal nodal Fermi velocity $v_{F,\mathrm{univ}} = (2.7 \pm 0.5) \times 10^5$ m/s for cuprate superconductors. These are the raw data reported by Zhou *et al.*[37] for $(La_{2-x}Sr_x)CuO_4$ (LSCO), $(La_{2-x-y}Nd_ySr_x)CuO_4$ (Nd-LSCO), $Bi_2Sr_2CaCu_2O_8$ (Bi-2212), $Bi_2Sr_2CuO_6$ (Bi-2201), $(Ca_{2-x}Na_x)CuO_2Cl_2$ (Na-CCOC), and $Tl_2Ba_2CuO_6$ (Tl-2201).

of whether these materials also comply with other scaling laws for superconductors[44,45] requires more experimental data on normal-state resistivity $\rho(T)$[31,46–48] and ground-state London penetration depth $\lambda(0)$.[1,49,50]

Here, we report the results of our search for a universal Fermi velocity in NRTS materials, based on an analysis of the full inventory of values for the ground-state upper critical field $B_{c2}(0)$ in these materials. We find that a universal Fermi velocity, $v_{F,\mathrm{univ}}$, does indeed exist in NRTS materials and obeys the empirical law

$$v_{F,\mathrm{univ}} = \frac{1}{1.3} \times \frac{2\Delta(0)}{k_B T_c} \times 10^5 \text{ m/s}, \tag{2}$$

where k_B is Boltzmann's constant and $\Delta(0)$ is the ground-state superconducting energy gap.

II. DESCRIPTION OF APPROACH

In the Bardeen–Cooper–Schieffer (BCS) theory of superconductivity,[51] the ground-state coherence length $\xi(0)$ and the amplitude of the ground-state energy gap $\Delta(0)$ are linked through the expression

$$\xi(0) = \frac{\hbar v_F}{\pi \Delta(0)}, \tag{3}$$

where $\hbar$ is the reduced Planck's constant. BCS theory also involves a dimensionless ratio

$$\alpha = \frac{2\Delta(0)}{k_B T_c}. \tag{4}$$

Substitution of Eqs. (3) and (4) into Eq. (1) gives the dependence of the ground-state upper critical field on the transition temperature:

$$B_{c2}(0) = \left[\frac{\pi \phi_0 k_B^2}{8\hbar^2}\right] \frac{\alpha^2}{v_F^2} T_c^2, \tag{5}$$

where the multiplicative prefactor in square brackets is a constant:

$$A = \left[\frac{\pi \phi_0 k_B^2}{8\hbar^2}\right] = 1.38 \times 10^7 \text{ T m}^2/(\text{s}^2 \text{ K}^2). \tag{6}$$

Thus, if hydrogen-rich superconductors exhibit a universal Fermi velocity $v_{F,\mathrm{univ}}$, then a fit of the full inventory of the $B_{c2}(0)$ vs T_c dataset to the equation

$$B_{c2}(0) = A f T_c^{\beta}, \tag{7}$$

where β and $f = \alpha^2/v_F^2$ are free fitting parameters, should reveal that

$$\beta \cong 2, \tag{8}$$

and, if this is the case, then the universal Fermi velocity $v_{F,\mathrm{univ}}$ can be calculated from the deduced free-fitting parameter f as

$$v_{F,\mathrm{univ}} = \frac{\alpha}{\sqrt{f}} = \frac{1}{\sqrt{f}} \frac{2\Delta(0)}{k_B T_c}. \tag{9}$$

It should be noted that $\alpha = 2\Delta(0)/k_B T_c$ in highly compressed hydrogen-rich superconductors varies within the range[4,8,12,27,42,49,52–55]

$$3.2 \le \frac{2\Delta(0)}{k_B T_c} \le 5, \tag{10}$$

where the lower limit is the value deduced from experiment[42,50,52] and the upper limit is based on the many results obtained from first-principles calculations, which always predict $4.3 \le 2\Delta(0)/k_B T_c$ in NRTS materials,[4,8,12,27,53–55] including very high values of $2\Delta(0)/k_B T_c \cong 5.0$ for some NRTS phases.[4,8,12,27]

III. EXTRAPOLATION MODEL FOR THE GROUND-STATE UPPER CRITICAL FIELD

Equation (7) has the ground-state upper critical field $B_{c2}(0)$ as dependent variable. However, it is important to note that this value can be determined by the use of several extrapolative models[56–59] that utilize experimental $B_{c2}(T)$ data measured at high reduced temperatures T/T_c. The primary reason why there is a necessity for extrapolative models is that all highly compressed hydrogen-rich superconductors have $B_{c2}(T \to 0\text{ K}) > 20$ T, which cannot be measured by the conventional and widely used Physical Property Measurement System (manufactured by Quantum Design), for which the highest measurable magnetic field B_{appl} = 9–16 T (depending on the specific model). It should be also stressed that $B_{c2}(T \to 0\text{ K})$ for the NRTS compounds H_3S, LaH_{10}, YH_6/YH_9 and $(La,Y)H_{10}$ are so high that even measurements at the best available quasi-DC magnetic field facilities worldwide[31,48,60] cover only the range of reduced temperatures $\frac{1}{2} \lesssim T/T_c$.

In this paper, from the several extrapolative $B_{c2}(T)$ models that are available,[56–59] we use the following analytical approximate expression from Werthamer–Helfand–Hohenberg (WHH) theory,[61,62] which was proposed by Baumgartner *et al.*:[59]

$$B_{c2}(T) = \frac{1}{0.693}\frac{\phi_0}{2\pi\xi^2(0)}\left[\left(1-\frac{T}{T_c}\right) - 0.153\left(1-\frac{T}{T_c}\right)^2 - 0.152\left(1-\frac{T}{T_c}\right)^4\right], \quad (11)$$

where $\xi(0)$ and $T_c \equiv T_c(B = 0)$ are two free fitting parameters (this equation is referred to as the B-WHH model hereinafter). Equation (11) was originally proposed for the extrapolation of $B_{c2}(T)$ data for neutron-irradiated Nb_3Sn alloys,[59] and recently several research groups have found that provides good approximations for a variety of superconducting materials.[4,63–68] On this basis, in the present study, we used Eq. (11) as a good, robust and simple analytical tool to extrapolate the $B_{c2}(T)$ curve to the low-temperature high-field region.

It is a necessary to describe the criterion for extracting $B_{c2}(T)$ datasets from experimentally measured $R(T, B_{appl})$ curves. Several criteria are available for the definitions of T_c, $B_{c2}(T)$, and $T_c(B_{appl})$, which have been discussed recently for the case of NRTS in Ref. 69. We have found[69,70] that the best match between the electron–phonon coupling constant $\lambda_{e\text{–}ph}$ extracted from $R(T, B_{appl} = 0)$ curves and the $\lambda_{e\text{–}ph}$ computed by first-principles calculation is obtained when T_c is defined at a value of the ratio $R(T)/R_{norm}$ that is as low as practically possible (where R_{norm} is the normal-state resistance just above the transition). By analyzing the full inventory of $R(T, B_{appl})$ data for NRTS materials herein, we have come to the conclusion that owing to noise and slope issues with real-world $R(T, B_{appl})$ curves and the fact that highly compressed superhydrides contain several superconducting phases, the appropriate criterion is

$$\frac{R(T, B_{appl})}{R(T_c^{onset}, B_{appl})} = 0.05, \quad (12)$$

and we use this henceforth in this study.

IV. RESULTS

A. Unannealed highly compressed sulfur hydride

In the first paper on NRTS superconductors, Drozdov *et al.*[1] reported $R(T, B_{appl})$ data for unannealed highly compressed sulfur hydride (P = 155 GPa) in their Fig. 3(a). By using the criterion of Eq. (12) [which is $R(T, B_{appl})_{criterion}$ = 23 mΩ for the $R(T, B_{appl})$ curves shown in bottom insert in Fig. 3(a) in Ref. 1], we extracted the $B_{c2}(T)$ dataset for this sample, which is shown in Fig. 2. Because this $B_{c2}(T)$ dataset covers a significant part of the full temperature range 0 K < $T \le T_c$, there was no need to use an extrapolative fit, and instead we fitted this dataset to the model in Ref. 52, which allowed to

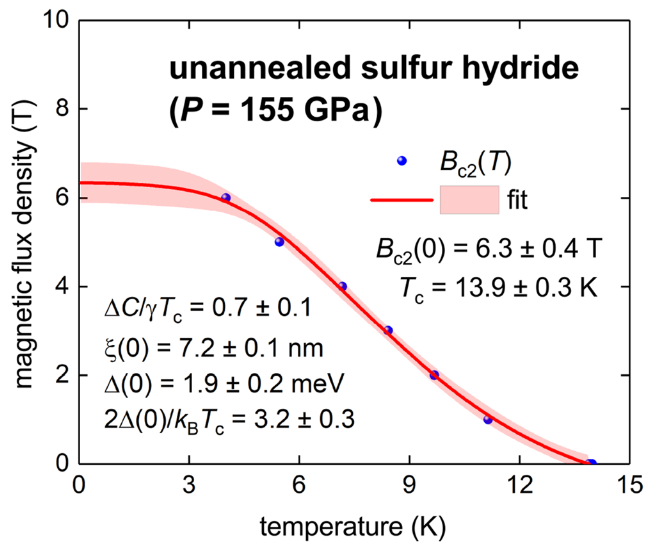

FIG. 2. Upper critical field data $B_{c2}(T)$ and data fit to Eqs. (13) and (14) for unannealed highly compressed sulfur hydride (P = 190 GPa). The raw $R(T, B_{appl})$ dataset was that reported by Drozdov *et al.*[1] The deduced values of $\xi(0)$, $\Delta(0)$, T_c, and $\Delta C/\gamma T_c$ are shown on the figure. The 95% confidence bands are shown by the pink shaded area. The fit quality is R = 0.9985.

deduce $\Delta(0)$, $2\Delta(0)/k_B T_c$, and $\Delta C/\gamma T_c$ (the last of which is the relative jump in electronic specific heat at T_c, with γ being the so-called Sommerfeld constant):

$$B_{c2}(T) = \frac{\phi_0}{2\pi\xi^2(0)}\left[\frac{1.77 - 0.43\left(\frac{T}{T_c}\right)^2 + 0.07\left(\frac{T}{T_c}\right)^4}{1.77}\right]^2 \times \left\{1 - \frac{1}{2k_B T}\int_0^\infty \frac{d\varepsilon}{\cosh^2\left[\frac{\sqrt{\varepsilon^2+\Delta^2(T)}}{2k_B T}\right]}\right\}, \quad (13)$$

where the temperature-dependent superconducting gap $\Delta(T)$ is given by[71,72]

$$\Delta(T) = \Delta(0)\tanh\left[\frac{\pi k_B T_c}{\Delta(0)}\sqrt{\eta\frac{\Delta C}{\gamma T_c}\left(\frac{T_c}{T} - 1\right)}\right], \quad (14)$$

with η = 2/3 for *s*-wave superconductors.

We used Eqs. (13) and (14) to extract $\xi(0)$, $\Delta(0)$, T_c, and $\Delta C/\gamma T_c$ from $B_{c2}(T)$ datasets for a variety of superconductors, including two highly compressed hydride phases of H_3S,[52] SnH_{12},[42] V_3Si,[73] and several iron-based superconductors.[73] However, it should be stressed that the approach using Eqs. (13) and (14) is only applicable for $B_{c2}(T)$ datasets defined by Eq. (12) or by a stricter criterion.

One of the most important deduced parameters, $\alpha = 2\Delta(0)/k_B T_c = 3.2 \pm 0.3$, is in remarkable agreement with the corresponding values deduced for highly compressed annealed H_3S (P = 155–160 GPa), $\alpha = 3.20 \pm 0.02$[49] and 3.55 ± 0.31,[52] and for highly compressed annealed SnH_{12} (P = 190 GPa), $\alpha = 3.28 \pm 0.18$.[42] The deduced $\Delta C/\gamma T_c = 0.7 \pm 0.1$ is also below the weak-coupling limit of BCS theory $\Delta C/\gamma T_c = 1.43$, as is the corresponding value for the annealed H_3S material, $\Delta C/\gamma T_c = 1.2 \pm 0.3$.[52] It should be mentioned that to deduce $\Delta C/\gamma T_c$ with higher accuracy requires more $B_{c2}(T)$ data points, especially at $T \sim T_c$. The deduced $B_{c2}(0)$ and T_c are given in Table I.

B. Annealed highly compressed hydrides

We processed reported $R(T, B_{appl})$ datasets for several annealed highly compressed hydrides by using Eq. (12) to extract $B_{c2}(T)$ datasets. The obtained datasets were fitted to Eq. (11), and the deduced values are given in Table I. These materials are as follows:

1. Sulfur superhydride H_3S (P = 155 and 160 GPa), for which the raw data were reported by Mozaffari *et al.*[31]
2. Cerium superhydride CeH_n (P = 88, 137, and 139 GPa), for which the raw data were reported by Chen *et al.*[12]
3. Lanthanum superhydride LaH_{10} (P = 120, 136 GPa), for which the raw data were reported by Sun *et al.*[60]
4. Yttrium superhydride/superdeuteride YH_6/YD_6 (P = 172 and 200 GPa), for which the raw data were reported by Troyan *et al.*[4]
5. Lanthanum–yttrium superhydride $(La,Y)H_{10}$ (P = 182, 183, and 186 GPa), for which the raw data were reported by Semenok *et al.*[8]
6. Tin superhydride SnH_{12} (P = 190 GPa), for which the raw data were reported by Hong *et al.*[11]
7. Thorium superhydrides ThH_9 and ThH_{10} (P = 170 GPa), for which the raw data were reported by Semenok *et al.*[16]

The respective fits are shown in Figs. S1–S7 in the supplementary material.

C. Analysis of $B_{c2}(0)$ vs T_c for superhydride phases

All deduced $B_{c2}(0)$ and T_c values for superhydride phases are collected in Table I, where we have also added data for the Th_4H_{15} phase reported by Satterthwaite and Toepke.[74]

The full dataset from Table I is shown in Fig. 3, together with the fit to Eq. (7). Although this dataset has a large scatter, it can be seen in Fig. 3(a) that the free-fitting power-law exponent $\beta = 2.07 \pm 0.14$ is practically undistinguishable from the expected value $\beta \equiv 2$ [Eq. (5)]. When β is the free-fitting parameter [Fig. 3(a)], the deduced $f = (1.19 \pm 0.90) \times 10^{-10}$ s^2/m^2 has a large uncertainty. However, when β is fixed to 2 [Fig. 3(b)], the free-fitting parameter f can be deduced with high accuracy as

$$f = \frac{\alpha^2}{v_{F,\mathrm{univ}}^2} = (1.68 \pm 0.08) \times 10^{-10}\ \mathrm{s^2/m^2}, \quad (15)$$

from which we can obtain

$$v_{F,\mathrm{univ}} = \frac{\alpha}{1.30 \pm 0.03} \times 10^5\ \mathrm{m/s} \cong \frac{1}{1.3} \times \frac{2\Delta(0)}{k_B T_c} \times 10^5\ \mathrm{m/s}. \quad (16)$$

By substituting the lower $[2\Delta(0)/k_B T_c = 3.2]$ and upper $[2\Delta(0)/k_B T_c = 5.0]$ limits of the ratio $2\Delta(0)/k_B T_c$ [Eq. (10)] into Eq. (16), we can establish the lower and upper limits of $v_{F,\mathrm{univ}}$ in superhydrides:

$$2.5 \times 10^5\ \mathrm{m/s} \lesssim v_{F,\mathrm{univ}} \lesssim 3.8 \times 10^5\ \mathrm{m/s}. \quad (17)$$

The deduced $v_{F,\mathrm{univ}}$ for hydrogen-rich superconductors [Eq. (16)] is similar to the corresponding value for high-T_c cuprates, $v_{F,\mathrm{univ}} = (2.7 \pm 0.5) \times 10^5$ m/s,[37] if Eq. (10) is taken into account.

TABLE I. Deduced $B_{c2}(0)$ and T_c values for hydrogen-rich superconductors for which raw $R(T, B_{appl})$ data are available to date.

Phase and data source	Figures	Pressure (GPa)	T_c (K)	ΔT_c (K)	$B_{c2}(0)$ (T)	$\Delta B_{c2}(0)$ (T)
Unannealed sulfur hydride [Fig. 3(a) in Ref. 1]	2	155	13.9	0.3	6.3	0.4
Annealed H_3S (Fig. 3 in Ref. 31)	S1(a)	155	185	2	98.8	1.2
Annealed H_3S (Figs. S1 and S2 in Ref. 31)	S1(b)	155	196.1	0.6	71.1	1.1
Annealed H_3S (Fig. 3 in Ref. 31)	S1(c)	160	143.9	1.4	59.2	2.3
Annealed CeH_9 [Fig. S7(a) in Ref. 12], cooling	S2(a)	88	38.8	0.4	16.5	1
Annealed CeH_9 [Fig. 1(c) in Ref. 12], warming	S2(b)	139	88.6	0.3	22.2	0.7
Annealed CeH_9 [Fig. 1(d) in Ref. 12], cooling	S2(c)	137	81.9	0.7	18.4	0.7
Annealed CeH_9 [Fig. 1(d) in Ref. 12], warming	S2(d)	137	82.7	0.7	18.7	0.6
Annealed LaH_{10} [Fig. 3(a) in Ref. 60]	S3(a)	120	174.8	0.8	90	3
Annealed LaH_{10} [Fig. 3(b) in Ref. 60]	S3(b)	136	206.2	0.8	136	3
Annealed YD_6 [Fig. S13(a) in Ref. 4]	S4(a)	172	157.7	0.2	124.9	2.4
Annealed YH_6 [Fig. S16(c) in Ref. 4]	S4(b)	200	206.2	0.2	97.2	1.4
Annealed $(La,Y)H_{10}$ [Fig. S27(b) in Ref. 8]	S5(a)	183	203.5	0.2	101.6	1.8
Annealed $(La,Y)H_{10}$ [Fig. S28(a) in Ref. 8]	S5(b)	182	234	0.1	135.8	1.5
Annealed $(La,Y)H_{10}$ [Fig. S28(a) in Ref. 8]	S5(c)	186	234.5	0.1	134	1
Annealed SnH_{12} [Fig. 4(a) in Ref. 11], cooling	S6(a)	190	62.8	0.4	9	0.2
Annealed SnH_{12} [Fig. 4(a) in Ref. 11], warming	S6(b)	190	64.1	0.5	8.9	0.2
Annealed ThH_9 [Fig. 4(a) in Ref. 16]	S7(a)	170	151.2	1.5	32	0.9
Annealed ThH_{10} [Fig. 4(a) in Ref. 16]	S7(b)	170	150.6	0.4	43.4	0.6
Th_4H_{15} (Ref. 74)		Ambient	8.2	0.15	2.75	0.25

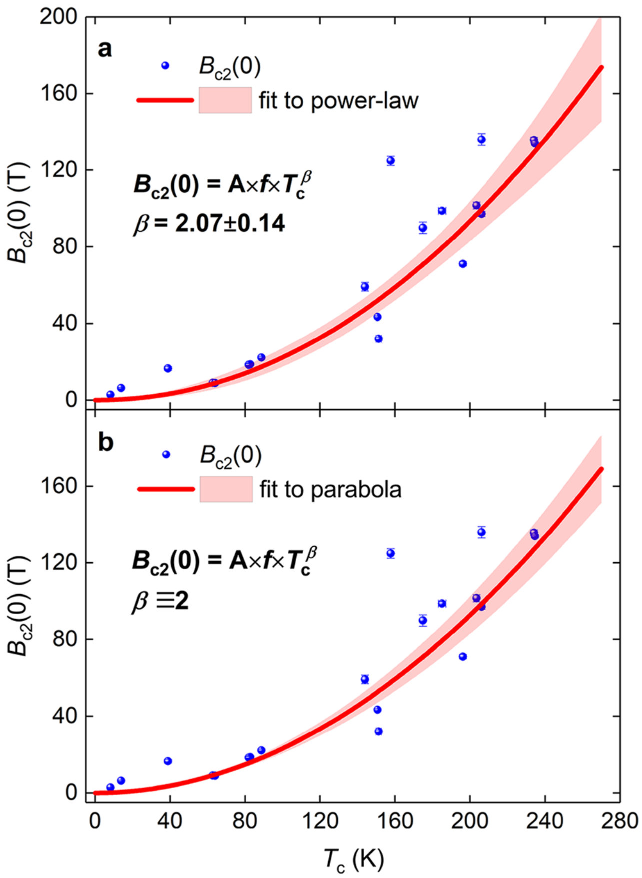

FIG. 3. Total $B_{c2}(0)$ vs T_c dataset for hydrogen-rich superconductors deduced in this work (Table I) and data fits to (a) Eq. (7) and (b) Eq. (5). (a) Free-fitting $\beta = 2.07 \pm 0.14$ and $f = (1.19 \pm 0.90) \times 10^{-10}$ s^2/m^2; the fit quality is $R = 0.9361$. (b) $\beta = 2.0$ (fixed) and free-fitting $f = (1.68 \pm 0.08) \times 10^{-10}$ s^2/m^2; the fit quality is $R = 0.9354$.

V. DISCUSSION

The primary assumption of the Migdal–Eliashberg (ME) theory of electron–phonon-mediated superconductivity[75–77] is that the ratio of characteristic phonon energy $\hbar\omega_D$ (where ω_D is the Debye frequency) to the Fermi energy E_F is very small, $\hbar\omega_D/E_F \ll 1$. In normal metals $\hbar\omega_D/E_F \lesssim 10^{-2}$,[78–82] and this is why ME theory is quantitatively accurate. However, for many high-temperature superconductors, the application of ME theory cannot be justified. In fact, in our previous studies,[69,70] we deduced the Debye temperature $T_\theta \cong 1500$ K, in highly compressed H_3S from a fit of experimentally measured temperature-dependent resistance $R(T)$ to the Bloch–Grüneisen equation.[83,84] This temperature can be converted into the Debye energy $k_B T_\theta = \hbar\omega_D \cong 0.13$ eV, and, considering that the Fermi energy was deduced in our previous study[52] as $E_F = 0.5$–1.0 eV, we can conclude that $0.13 \le \hbar\omega_D/E_F \le 0.26$, and thus ME theory[75,76] does not provide an exact description of highly compressed H_3S.

The first concern that nonadiabatic effects (i.e., effects beyond ME theory[75,76]) are important in highly compressed H_3S was expressed by Pietronero *et al.*,[82] who also pointed out that: "… *The fingerprints of non-adiabatic effects are: – position of the material in the Uemura diagram;…*" Although the traditional way to position a material in the Uemura plot requires knowledge of the ground-state London penetration depth $\lambda(0)$ (which has only recently been reported for H_3S[46]), the present author utilized the ground-state coherence length $\xi(0)$ [deduced from the $B_{c2}(T)$ data] and found[52] that H_3S falls into the unconventional superconductors band in the Uemura plot.[41] In later work,[42,85–88] it was established that LaH_{10}, Th_4H_{15}, ThH_9, ThH_{10}, YH_6, SH_{12}, and H_3(S,C) also fall into the unconventional superconductors band in the Uemura plot. This is direct evidence that the ratio $\hbar\omega_D/E_F$ in superhydrides has values well above those typical of conventional superconductors, $\hbar\omega_D/E_F \lesssim 10^{-2}$.

On the basis of the derived universal Fermi velocity in superhydrides, $v_{F,\mathrm{univ}}$ [Eq. (16)], we can conclude that the strength of the nonadiabatic effects in a superhydride (as quantified by the ratio $\hbar\omega_D/E_F$) can be revealed if the Debye temperature T_θ of the compound can be deduced from the normal part of the temperature-dependent resistance $R(T)$.[69,70,86] It should be noted that the Debye temperature in superhydrides varies from $T_\theta \cong 870$ K (D_3S, $P = 173$ GPa[69]) up to $T_\theta \cong 1700$ K ($R3m$-phase of H_3S, $P = 133$ GPa[69]).

An analysis of the first experimental $R(T)$ data[89] measured for metallic hydrogen phase III (compressed at $P = 402$ GPa) revealed that $T_\theta \cong 730$ K.[70] If we assume that metallic hydrogen phase III complies with the established $v_{F,\mathrm{univ}}$ [Eq. (16)] and that it has $2\Delta(0)/k_B T_c = 3.53$ and exhibits no effective mass enhancement, then the ratio $\hbar\omega_D/E_F$ can be estimated as $\hbar\omega_D/E_F = 0.3$. This implies that metallic hydrogen should exhibit pronounced nonadiabatic effects,[78–82] which could prevent the emergence of a superconducting state in this metal at high temperature.

It should be also mentioned that first principles calculations (FPC) are an essential part of current NRTS phase searches.[27] The accuracy and powerful capabilities of FPC became obvious after the pivotal prediction of the $Im\bar{3}m - H_3S$ phase,[90,91] which was later discovered experimentally.[1] Another achievement of the FPC approach was demonstrated recently when Li *et al.*[92] and Ma *et al.*[93] reported the discovery of a calcium superhydride phase with transition temperature $T_c = 200$–215 K (at a pressure $P = 160$–190 GPa), which was predicted by Wang *et al.*[94] in 2012. However, it should also be mentioned that the superconductivity predicted by FPC in some binary systems (e.g., AlH_3[95,96]), has never been observed experimentally. This implies that further development of FPC techniques to take account of non-adiabatic effects is highly desirable.

Overall, remarkable progress has been achieved in this field from the first theoretical predictions of high-temperature superconductivity in metallic hydrogen[97,98] and hydrogen-dominated alloys[74,99] five decades ago to the remarkable experimental and FPC results[1,27] reported recently. It should be stressed that all the primary discoveries in the field (e.g., the direct searches for and syntheses of the H_3S, LaH_{10}, and YH_6 phases) have come from a perfect conjunction of theory and experiment. An excellent example of this is the story of the discovery of near-room-temperature superconductivity in highly compressed sulfur hydride.[1] In February 2014, Li *et al.*[100] reported results of FPC calculations for highly compressed sulfur hydride. These calculations showed that at P = 160 GPa, the sulfur hydride retains the composition of H_2S and that this compound exhibits a superconducting transition temperature of $T_c \sim 80$ K. In November 2014, an alternative theoretical result was reported by Duan *et al.*,[91] who performed thorough FPC using USPEX software[101–103] and predicted that sulfur hydride would decompose into a mixture of elemental sulfur and an $(H_2S)_2H_2$ phase at high pressure. This result was in a good accord with an earlier report by Strobel *et al.*,[104] who showed experimentally that at $P > 3.2$ GPa, the H_2S–H_2 mixture exhibited structural ordering with the formation of the $(H_2S)_2H_2$ phase (with four formula units per unit cell). The predicted transition temperature for the $(H_2S)_2H_2$ phase was T_c = 191–204 K at P = 200 GPa.[91] On December 1, 2014, Drozdov *et al.*[105] reported a milestone experimental result on the observation of $T_c \approx 190$ K in sulfur hydride compressed at $P > 150$ GPa.

Another remarkable story should also be mentioned here, namely, the discovery of the $Fm\bar{3}m-LaH_{10}$ phase, for which $T_c \cong 274$–286 K at P = 210 GPa was theoretically predicted by Liu *et al.*[106] in June 2017. This NRTS phase was experimentally discovered by Drozdov *et al.*[107] on August 21, 2018, and, two days later, Somayazulu *et al.*[108] confirmed this discovery.

VI. CONCLUSIONS

In this study, we have proposed that hydrogen-rich superconductors exhibit a universal Fermi velocity v_F, which is given by empirical expression $v_{F,\mathrm{univ}} = (1/1.3) \times [2\Delta(0)/k_BT_c] \times 10^5$ m/s. Considering that the gap-to-transition temperature ratio $2\Delta(0)/k_BT_c$ in hydrogen-rich superconductors varies within the range $3.2 \le 2\Delta(0)/k_BT_c \le 5.0$, we conclude that $v_{F,\mathrm{univ}}$ varies within the range 2.5×10^5 m/s $\le v_{F,\mathrm{univ}} \le 3.8 \times 10^5$ m/s.

The Debye temperature T_θ can be deduced from the temperature-dependent resistance $R(T)$ of the conductor,[69,83,84] and so this universal Fermi velocity v_F in superhydrides [Eq. (16)] can be used to calculate the ratio $\hbar\omega_D/E_F$, which determines the strength of nonadiabatic effects in the superconductor. Calculations for metallic hydrogen phase III (compressed at P = 402 GPa) have shown that $\hbar\omega_D/E_F = 0.3$, which implies strong nonadiabatic effects in this metal.

SUPPLEMENTARY MATERIAL

See the supplementary material for the $B_{c2}(T)$ fits to Eq. (11) for highly compressed superhydrides.

ACKNOWLEDGMENTS

The author thanks Luciano Pietronero (Universita' di Roma) for comments about the limitations of the applicability of the Migdal–Eliashberg (ME) theory of electron–phonon-mediated superconductivity to high-temperature superconductors.

The author is grateful for financial support provided by the Ministry of Science and Higher Education of the Russian Federation through the theme "Pressure" Grant No. AAAA-A18-118020190104-3 and through a Ural Federal University project within the Priority-2030 Program.

AUTHOR DECLARATIONS

Conflict of Interest

The author has no conflicts to disclose.

Author Contributions

Evgeny F. Talantsev: Conceptualization (lead); Data curation (lead); Formal analysis (lead); Investigation (lead); Methodology (lead); Validation (lead); Visualization (lead); Writing – original draft (lead); Writing – review & editing (lead).

DATA AVAILABILITY

Data sharing is not applicable to this article as no new data were created or analyzed in this study.

REFERENCES

1 A. P. Drozdov, M. I. Eremets, I. A. Troyan, V. Ksenofontov, and S. I. Shylin, "Conventional superconductivity at 203 kelvin at high pressures in the sulfur hydride system," Nature **525**, 73–76 (2015).
2 A. P. Drozdov *et al.*, "Superconductivity at 250 K in lanthanum hydride under high pressures," Nature **569**, 528–531 (2019).
3 M. Somayazulu *et al.*, "Evidence for superconductivity above 260 K in lanthanum superhydride at megabar pressures," Phys. Rev. Lett. **122**, 027001 (2019).
4 I. A. Troyan *et al.*, "Anomalous high-temperature superconductivity in YH_6," Adv. Mater. **33**, 2006832 (2021).
5 P. Kong *et al.*, "Superconductivity up to 243 K in yttrium hydrides under high pressure," Nat. Commun. **12**, 5075 (2021).
6 L. Ma *et al.*, "High-temperature superconducting phase in clathrate calcium hydride CaH_6 up to 215 K at a pressure of 172 GPa," Phys. Rev. Lett. **128**, 167001 (2022).
7 C. L. Zhang *et al.*, "Superconductivity above 80 K in polyhydrides of hafnium," arXiv:2208.05816v1.
8 D. V. Semenok *et al.*, "Superconductivity at 253 K in lanthanum–yttrium ternary hydrides," Mater. Today **48**, 18–28 (2021).
9 D. Zhou *et al.*, "Superconducting praseodymium superhydrides," Sci. Adv. **6**, eaax6849 (2020).
10 T. Matsuoka *et al.*, "Superconductivity of platinum hydride," Phys. Rev. B **99**, 144511 (2019).
11 F. Hong *et al.*, "Possible superconductivity at ~70 K in tin hydride SnH_x under high pressure," Mater. Today Phys. **22**, 100596 (2022).
12 W. Chen, D. V. Semenok, X. Huang, H. Shu, X. Li, D. Duan, T. Cui, and A. R. Oganov, "High-temperature superconducting phases in cerium superhydride with a T_c up to 115 K below a pressure of 1 Megabar," Phys. Rev. Lett. **127**, 117001 (2021).
13 M. Sakata *et al.*, "Superconductivity of lanthanum hydride synthesized using AlH_3 as a hydrogen source," Supercond. Sci. Technol. **33**, 114004 (2020).
14 W. Chen *et al.*, "Synthesis of molecular metallic barium superhydride: Pseudocubic BaH_{12}," Nat. Commun. **12**, 273 (2021).
15 M. A. Kuzovnikov and M. Tkacz, "High-pressure synthesis of novel polyhydrides of Zr and Hf with a Th_4H_{15}-type structure," J. Phys. Chem. C **123**, 30059–30066 (2019).
16 D. V. Semenok *et al.*, "Superconductivity at 161 K in thorium hydride ThH_{10}: Synthesis and properties," Mater. Today **33**, 36–44 (2020).
17 N. N. Wang *et al.*, "A low-T_c superconducting modification of Th_4H_{15} synthesized under high pressure," Supercond. Sci. Technol. **34**, 034006 (2021).
18 A. P. Drozdov, M. I. Eremets, and I. A. Troyan, "Superconductivity above 100 K in PH3 at high pressures," arXiv:1508.06224.
19 M. Shao *et al.*, "Superconducting ScH_3 and LuH_3 at megabar pressures," Inorg. Chem. **60**, 15330 (2021).

[20]J. Chen *et al.*, "Computational design of novel hydrogen-rich YS–H compounds," ACS Omega **4**, 14317–14323 (2019).
[21]J. A. Alarco, P. C. Talbot, and I. D. R. Mackinnon, "Identification of superconductivity mechanisms and prediction of new materials using density functional theory (DFT) calculations," J. Phys.: Conf. Ser. **1143**, 012028 (2018).
[22]D. V. Semenok, A. G. Kvashnin, I. A. Kruglov, and A. R. Oganov, "Actinium hydrides AcH_{10}, AcH_{12}, and AcH_{16} as high-temperature conventional superconductors," J. Phys. Chem. Lett. **9**, 1920–1926 (2018).
[23]C. J. Pickard, I. Errea, and M. I. Eremets, "Superconducting hydrides under pressure," Annu. Rev. Condens. Matter Phys. **11**, 57–76 (2020).
[24]J. A. Flores-Livas, L. Boeri, A. Sanna, G. Profeta, R. Arita, and M. Eremets, "A perspective on conventional high-temperature superconductors at high pressure: Methods and materials," Phys. Rep. **856**, 1–78 (2020).
[25]A. Goncharov, "Phase diagram of hydrogen at extreme pressures and temperatures; updated through 2019 (Review article)," Low Temp. Phys. **46**, 97 (2020).
[26]E. Gregoryanz, C. Ji, P. Dalladay-Simpson, B. Li, R. T. Howie, and H.-K. Mao, "Everything you always wanted to know about metallic hydrogen but were afraid to ask," Matter Radiat. Extremes **5**, 038101 (2020).
[27]B. Lilia *et al.*, "The 2021 room-temperature superconductivity roadmap," J. Phys.: Condens. Matter **34**, 183002 (2022).
[28]X. Zhang, Y. Zhao, and G. Yang, "Superconducting ternary hydrides under high pressure," Wiley Interdiscip. Rev.: Comput. Mol. Sci. **12**, e1582 (2021).
[29]M. Dogan and M. L. Cohen, "Anomalous behaviour in high-pressure carbonaceous sulfur hydride," Physica C **583**, 1353851 (2021).
[30]T. Wang *et al.*, "Absence of conventional room temperature superconductivity at high pressure in carbon doped H_3S," Phys. Rev. B **104**, 064510 (2021).
[31]S. Mozaffari *et al.*, "Superconducting phase diagram of H_3S under high magnetic fields," Nat. Commun. **10**, 2522 (2019).
[32]V. S. Minkov, V. B. Prakapenka, E. Greenberg, and M. I. Eremets, "A boosted critical temperature of 166 K in superconducting D_3S synthesized from elemental sulfur and hydrogen," Angew. Chem., Int. Ed. **59**, 18970–18974 (2020).
[33]R. Matsumoto *et al.*, "Electrical transport measurements for superconducting sulfur hydrides using boron-doped diamond electrodes on beveled diamond anvil," Supercond. Sci. Technol. **33**, 124005 (2020).
[34]D. Laniel *et al.*, "Novel sulfur hydrides synthesized at extreme conditions," Phys. Rev. B **102**, 134109 (2020).
[35]X. Huang *et al.*, "High-temperature superconductivity in sulfur hydride evidenced by alternating-current magnetic susceptibility," Natl. Sci. Rev. **6**, 713–718 (2019).
[36]V. L. Ginzburg and L. D. Landau, Z. Eksp. Teor. Fiz. **20**, 1064 (1950).
[37]X. J. Zhou *et al.*, "High-temperature superconductors: Universal nodal Fermi velocity," Nature **423**, 398 (2003).
[38]D. K. Sunko, "High-temperature superconductors as ionic metals," J. Supercond. Novel Magn. **33**, 27–33 (2020).
[39]D. R. Harshman and A. T. Fiory, "High-T_c superconductivity in hydrogen clathrates mediated by Coulomb interactions between hydrogen and central-atom electrons," J. Supercond. Novel Magn. **33**, 2945–2961 (2020).
[40]D. R. Harshman and A. T. Fiory, "The superconducting transition temperatures of C–S–H based on inter-sublattice S–H_4-tetrahedron electronic interactions," J. Appl. Phys. **131**, 015105 (2022).
[41]Y. J. Uemura, "Bose-Einstein to BCS crossover picture for high-T_c cuprates," Physica C **282-287**, 194–197 (1997).
[42]E. F. Talantsev, "Comparison of highly-compressed $C2/m$-SnH_{12} superhydride with conventional superconductors," J. Phys.: Condens. Matter **33**, 285601 (2021).
[43]E. F. Talantsev, W. P. Crump, and J. L. Tallon, "Universal scaling of the self-field critical current in superconductors: From sub-nanometre to millimetre size," Sci. Rep. **7**, 10010 (2017).
[44]C. C. Homes, S. V. Dordevic, M. Strongin, D. A. Bonn, R. Liang, W. N. Hardy, S. Komiya, Y. Ando, G. Yu, N. Kaneko, X. Zhao, M. Greven, D. N. Basov, and T. Timusk, "A universal scaling relation in high-temperature superconductors," Nature **430**, 539–541 (2004).
[45]M. R. Koblischka and A. Koblischka-Veneva, "Calculation of T_c of superconducting elements with the Roeser–Huber formalism," Metals **12**, 337 (2022).
[46]M. I. Eremets, V. S. Minkov, A. P. Drozdov, P. P. Kong, V. Ksenofontov, S. I. Shylin, S. L. Bud'ko, R. Prozorov, F. F. Balakirev, D. Sun, S. Mozaffari, and L. Balicas, "High-temperature superconductivity in hydrides: Experimental evidence and details," J. Supercond. Novel Magn. **35**, 965–977 (2022).
[47]I. Osmond, O. Moulding, S. Cross, T. Muramatsu, A. Brooks, O. Lord, T. Fedotenko, J. Buhot, and S. Friedemann, "Clean-limit superconductivity in $Im\bar{3}m$ H_3S synthesized from sulfur and hydrogen donor ammonia borane," Phys. Rev. B **105**, L220502 (2022).
[48]D. V. Semenok *et al.*, "Effect of magnetic impurities on superconductivity in LaH_{10}," Adv. Mater. (published online) (2022).
[49]E. F. Talantsev, W. P. Crump, J. G. Storey, and J. L. Tallon, "London penetration depth and thermal fluctuations in the sulphur hydride 203 K superconductor," Ann. Phys. **529**, 1600390 (2017).
[50]V. S. Minkov, S. L. Bud'ko, F. F. Balakirev, V. B. Prakapenka, S. Chariton, R. J. Husband, H. P. Liermann, and M. I. Eremets, "Magnetic field screening in hydrogen-rich high-temperature superconductors," Nat. Commun. **13**, 3194 (2022).
[51]J. Bardeen, L. N. Cooper, and J. R. Schrieffer, "Theory of superconductivity," Phys. Rev. **108**, 1175–1204 (1957).
[52]E. F. Talantsev, "Classifying superconductivity in compressed H_3S," Mod. Phys. Lett. B **33**, 1950195 (2019).
[53]I. Errea *et al.*, "Quantum crystal structure in the 250-kelvin superconducting lanthanum hydride," Nature **578**, 66–69 (2020).
[54]C. Heil, S. di Cataldo, G. B. Bachelet, and L. Boeri, "Superconductivity in sodalite-like yttrium hydride clathrates," Phys. Rev. B **99**, 220502(R) (2019).
[55]J. A. Camargo-Martínez *et al.*, "The higher superconducting transition temperature T_c and the functional derivative of T_c with $\alpha^2F(\omega)$ for electron–phonon superconductors," J. Phys.: Condens. Matter **32**, 505901 (2020).
[56]C. J. Gorter and H. Casimir, "On supraconductivity I," Physica **1**, 306–320 (1934).
[57]C. K. Jones, J. K. Hulm, and B. S. Chandrasekhar, "Upper critical field of solid solution alloys of the transition elements," Rev. Mod. Phys. **36**, 74 (1964).
[58]L. P. Gor'kov, "The critical supercooling field in superconductivity theory," Sov. Phys. JETP **10**, 593–599 (1960).
[59]T. Baumgartner, M. Eisterer, H. W. Weber, R. Flükiger, C. Scheuerlein, and L. Bottura, "Effects of neutron irradiation on pinning force scaling in state-of-the-art Nb_3Sn wires," Supercond. Sci. Technol. **27**, 015005 (2014).
[60]D. Sun *et al.*, "High-temperature superconductivity on the verge of a structural instability in lanthanum superhydride," Nat. Commun. **12**, 6863 (2021).
[61]E. Helfand and N. R. Werthamer, "Temperature and purity dependence of the superconducting critical field, H_{c2}. II," Phys. Rev. **147**, 288–294 (1966).
[62]N. R. Werthamer, E. Helfand, and P. C. Hohenberg, "Temperature and purity dependence of the superconducting critical field, H_{c2}. III. Electron spin and spin-orbit effects," Phys. Rev. **147**, 295–302 (1966).
[63]H. Ninomiya *et al.*, "Superconductivity in a scandium borocarbide with a layered crystal structure," Inorg. Chem. **58**, 15629–15636 (2019).
[64]H. Xie *et al.*, "Superconducting zirconium polyhydrides at moderate pressures," J. Phys. Chem. Lett. **11**, 646–651 (2020).
[65]W. Zhang *et al.*, "A new superconducting 3R-WS_2 phase at high pressure," J. Phys. Chem. Lett. **12**, 3321–3327 (2021).
[66]M. Scuderi *et al.*, "Nanoscale analysis of superconducting Fe(Se,Te) epitaxial thin films and relationship with pinning properties," Sci. Rep. **11**, 20100 (2021).
[67]K. Ma *et al.*, "Group-9 transition-metal suboxides adopting the filled-Ti_2Ni structure: A class of superconductors exhibiting exceptionally high upper critical fields," Chem. Mater. **33**, 8722–8732 (2021).
[68]M. Boubeche *et al.*, "Enhanced superconductivity with possible re-appearance of charge density wave states in polycrystalline $Cu_{1-x}Ag_xIr_2Te_4$ alloys," J. Phys. Chem. Solids **163**, 110539 (2022).
[69]E. F. Talantsev, "Advanced McMillan's equation and its application for the analysis of highly-compressed superconductors," Supercond. Sci. Technol. **33**, 094009 (2020).
[70]E. F. Talantsev, "The electron–phonon coupling constant and the Debye temperature in polyhydrides of thorium, hexadeuteride of yttrium, and metallic hydrogen phase III," J. Appl. Phys. **130**, 195901 (2021).

[71] F. Gross *et al.*, "Anomalous temperature dependence of the magnetic field penetration depth in superconducting UBe_{13}," Z. Phys. B: Condens. Matter **64**, 175–188 (1986).

[72] F. Groß-Alltag, B. S. Chandrasekhar, D. Einzel, P. J. Hirschfeld, and K. Andres, "London field penetration in heavy fermion superconductors," Z. Phys. B: Condens. Matter **82**, 243–255 (1991).

[73] E. F. Talantsev, "In-plane *p*-wave coherence length in iron-based superconductors," Results Phys. **18**, 103339 (2020).

[74] C. B. Satterthwaite and I. L. Toepke, "Superconductivity of hydrides and deuterides of thorium," Phys. Rev. Lett. **25**, 741–743 (1970).

[75] A. B. Migdal, "Interaction between electrons and lattice vibrations in a normal metal," Sov. Phys. JETP **7**, 996–1001 (1958).

[76] G. M. Eliashberg, "Interactions between electrons and lattice vibrations in a superconductor," Sov. Phys. JETP **11**, 696–702 (1960).

[77] F. Marsiglio, "Eliashberg theory: A short review," Ann. Phys. **417**, 168102 (2020).

[78] L. Pietronero, S. Strässler, and C. Grimaldi, "Nonadiabatic superconductivity. I. Vertex corrections for the electron-phonon interactions," Phys. Rev. B **52**, 10516–10529 (1995).

[79] C. Grimaldi, L. Pietronero, and S. Strässler, "Nonadiabatic superconductivity. II. Generalized Eliashberg equations beyond Migdal's theorem," Phys. Rev. B **52**, 10530–10546 (1995).

[80] C. Grimaldi, E. Cappelluti, and L. Pietronero, "Isotope effect on m^* in high T_c materials due to the breakdown of Migdal's theorem," Europhys. Lett. **42**, 667 (1998).

[81] E. Cappelluti, S. Ciuchi, C. Grimaldi, L. Pietronero, and S. Strässler, "High T_c superconductivity in MgB_2 by nonadiabatic pairing," Phys. Rev. Lett. **88**, 117003 (2002).

[82] L. Pietronero, L. Boeri, E. Cappelluti, and L. Ortenzi, "Conventional/unconventional superconductivity in high-pressure hydrides and beyond: Insights from theory and perspectives," Quantum Stud.: Math. Found. **5**, 5–21 (2018).

[83] F. Bloch, "Zum elektrischen widerstandsgesetz bei tiefen temperaturen," Z. Phys. **59**, 208–214 (1930).

[84] F. J. Blatt, *Physics of Electronic Conduction in Solids* (McGraw-Hill, New York, 1968), pp. 185–190.

[85] E. F. Talantsev, "Classifying hydrogen-rich superconductors," Mater. Res. Express **6**, 106002 (2019).

[86] E. F. Talantsev, "An approach to identifying unconventional superconductivity in highly-compressed superconductors," Supercond. Sci. Technol. **33**, 124001 (2020).

[87] E. F. Talantsev and R. C. Mataira, "Classifying superconductivity in ThH-ThD superhydrides/superdeuterides," Mater. Res. Express **7**, 016003 (2020).

[88] E. F. Talantsev, "The electron-phonon coupling constant, Fermi temperature and unconventional superconductivity in the carbonaceous sulfur hydride 190 K superconductor," Supercond. Sci. Technol. **34**, 034001 (2021).

[89] M. I. Eremets, P. P. Kong, and A. P. Drozdov, "Metallization of hydrogen," arXiv:2109.11104 (2021).

[90] Y. Li, J. Hao, H. Liu, Y. Li, and Y. Ma, "The metallization and superconductivity of dense hydrogen sulfide," J. Chem. Phys. **140**, 174712 (2014).

[91] D. Duan, Y. Liu, F. Tian, D. Li, X. Huang, Z. Zhao, H. Yu, B. Liu, W. Tian, and T. Cui, "Pressure-induced metallization of dense $(H_2S)_2H_2$ with high-T_c superconductivity," Sci. Rep. **4**, 6968 (2014).

[92] Z. Li *et al.*, "Superconductivity above 200 K discovered in superhydrides of calcium," Nat. Commun. **13**, 2863 (2022); arXiv:2103.16917.

[93] L. Ma, K. Wang, Y. Xie, X. Yang, Y. Wang, M. Zhou, H. Liu, X. Yu, Y. Zhao, H. Wang, G. Liu, and Y. Ma, "High-temperature superconducting phase in clathrate calcium hydride CaH_6 up to 215 K at a pressure of 172 GPa," Phys. Rev. Lett. **128**, 167001 (2022).

[94] H. Wang, J. S. Tse, K. Tanaka, T. Iitaka, and Y. Ma, "Superconductive sodalite-like clathrate calcium hydride at high pressures," Proc. Natl. Acad. Sci. U. S. A. **109**, 6463–6466 (2012).

[95] I. Goncharenko, M. I. Eremets, M. Hanfland, J. S. Tse, M. Amboage, Y. Yao, and I. A. Trojan, "Pressure-induced hydrogen-dominant metallic state in aluminum hydride," Phys. Rev. Lett. **100**, 045504 (2008).

[96] P. Hou, F. Belli, R. Bianco, and I. Errea, "Strong anharmonic and quantum effects in $Pm\bar{3}n$ AlH_3 under high pressure: A first-principles study," Phys. Rev. B **103**, 134305 (2021).

[97] N. W. Ashcroft, "Metallic hydrogen: A high-temperature superconductor?," Phys. Rev. Lett. **21**, 1748–1749 (1968).

[98] V. L. Ginzburg, "Superfluidity and superconductivity in the universe," J. Stat. Phys. **1**, 3–24 (1969).

[99] J. F. Miller, R. H. Caton, and C. B. Satterthwaite, "Low-temperature heat capacity of normal and superconducting thorium hydride and thorium deuteride," Phys. Rev. B **14**, 2795 (1976).

[100] Y. Li, J. Hao, Y. Li, and Y. Ma, "The metallization and superconductivity of dense hydrogen sulphide," arXiv:1402.2721 (2014).

[101] A. R. Oganov and C. W. Glass, "Crystal structure prediction using *ab initio* evolutionary techniques: Principles and applications," J. Chem. Phys. **124**, 244704–244715 (2006).

[102] A. R. Oganov, A. O. Lyakhov, and M. Valle, "How evolutionary crystal structure prediction works—And why," Acc. Chem. Res. **44**, 227–237 (2011).

[103] A. O. Lyakhov, A. R. Oganov, H. T. Stokes, and Q. Zhu, "New developments in evolutionary structure prediction algorithm USPEX," Comput. Phys. Commun. **184**, 1172–1182 (2013).

[104] T. A. Strobel, P. Ganesh, M. Somayazulu, P. R. C. Kent, and R. J. Hemley, "Novel cooperative interactions and structural ordering in H_2S–H_2," Phys. Rev. Lett. **107**, 255503 (2011).

[105] A. P. Drozdov, M. I. Eremets, and I. A. Troyan, "Conventional superconductivity at 190 K at high pressures," arXiv:1412.0460 (2014).

[106] H. Liu, I. I. Naumov, R. Hoffmann, N. W. Ashcroft, and R. J. Hemley, "Potential high-T_c superconducting lanthanum and yttrium hydrides at high pressure," Proc. Natl. Acad. Sci. U. S. A. **114**, 6990–6995 (2017).

[107] A. P. Drozdov, V. S. Minkov, S. P. Besedin, P. P. Kong, M. A. Kuzovnikov, D. A. Knyazev, and M. I. Eremets, "Superconductivity at 215 K in lanthanum hydride at high pressures," arXiv:1808.07039 (2018).

[108] M. Somayazulu, M. Ahart, A. K. Mishra, Z. M. Geballe, M. Baldini, Y. Meng, V. V. Struzhkin, and R. J. Hemley, "Evidence for superconductivity above 260 K in lanthanum superhydride at megabar pressures," arXiv:1808.07695 (2018).